Journal of Physics: Conference Series **190** (2009) 012123 doi:10.1088/1742-6596/190/1/012123

Temperature dependence of EXAFS cumulants of Ag nanoparticles in glass

M Dubiel[1], J Haug[1], H Kruth[1], H Hofmeister[2] and W Seifert[1]
[1]Department of Physics, University of Halle-Wittenberg, Friedemann-Bach-Platz 6, D-06108 Halle, Sachsen-Anhalt, Germany
[2]Max Planck Institute of Microstructure Physics, D-06120 Halle, Germany

E-mail: manfred.dubiel@physik.uni-halle.de

Abstract. Ag nanoparticles of 1.5 to 7 nm size were produced by ion exchange of soda-lime glass for various duration. Information on local order and thermal vibrations were available by means of X-ray absorption spectroscopy using experiments at the Ag K-edge (25.514 keV). Ratio method and EXAFS fitting procedure were successfully applied to reveal the temperature dependence using the cumulant-expansion method up to third order ones. The temperature dependence of the nearest neighbor Ag-Ag distance appears different from that of polycrystalline Ag foil below 400 K. This effect can be explained by a thermoelastic model describing the mismatch of thermal expansion coefficients of Ag particles and the glass matrix. In addition, the parameter of Ag-Ag bond length of 1.5 nm particles is governed by precursor formation for crystalline Ag nanoparticles. The data of the second cumulant, the Debye-Waller factor (DWF), represent a higher static disorder, especially for nanoparticles of 1.5 – 3.5 nm size, caused by the increasing portion of surface or interface atoms. From the temperature dependent part of DWF we estimated a slightly increased Einstein temperature.

1. Introduction

Nanosized particles embedded in glass have attracted much interest as material with potential applications because of specific linear and non-linear optical properties [1], where strong variations are expected for sizes, i. e. particle diameters, much less than 10 nm. Therefore, we used ion exchange processing to produce Ag nanoparticles in commercial soda-lime glass with sizes of 1 to 7 nm. Because of these small dimensions specific experimental methods for identification and characterization of such species were needed, in particular for particles embedded in a disordered matrix like glass. Extended X-ray absorption fine structure (EXAFS) spectroscopy is a powerful tool to characterize the local order around atoms together with the thermal vibrations and the static disorder in crystalline as well as in disordered or amorphous materials. For nanoparticles and clusters, there are no limitations with respect to their size [2,3]. The present work is aimed at investigating the structural and vibrational behaviour of silver particles in ion-exchanged glass in dependence on particle size and temperature. The EXAFS data like Ag-Ag distance, Debye-Waller factor and higher cumulants should allow to clarify the influence of quantum size effects, interaction between particles and surrounding matrix as well as thermal effects induced by preparation at elevated temperatures.

2. Experimental and data evaluation

Commercial soda-lime glass containing (in weight %) 71.9% SiO_2 and 13.3% Na_2O as main components and 0.865% Fe_2O_3 as Fe ion component acting as reducing agent was used as base glass

material. The Ag ions were incorporated by immersing the samples into $NaNO_3/AgNO_3$ mixed melt at 330°C for various duration. At this temperature, the formation of crystalline nuclei or small nanoscaled particles should be favoured. Transmission electron microscopy (TEM) examination to evaluate size and size distribution of silver particles was done by means of JEM 1010 operating at 100 kV. To this aim both, planar and cross-section preparation, were performed including mechanical grinding, polishing and ion-beam etching. By TEM a mean particle size of 1.5 nm for an ion exchange duration in the range of 100 to 400 hours was found [4]. Upon longer ion exchange, or upon subsequent heat treatment above 400°C distinct particle growth could be observed. Thus, mean particle sizes between 2 and 7 nm were obtained. The distribution of sizes for all samples is nearly symmetric. The uncertainty of sizes is given by a standard deviation between 1.3 and 1.5 nm.
Ag K-spectra (25.514 keV) were recorded in transmission mode at 10 K by means of a liquid-helium vapour flow cryostat at beam line X1 and A1 at HASYLAB, respectively. EXAFS data processing was done using the UWXAFS program package [5], including background subtraction, Fourier transformation of the extracted EXAFS oscillations into real space and subsequent fitting in real space (0.16-04 nm) with the theoretical amplitude and phase functions using FEFF 8 [6]. For evaluation of experimental data, in addition to the interatomic distance and the Debye-Waller factor $C_2 = \sigma^2$, the third and fourth cumulants, C_3 and C_4, were also taken into consideration. In addition, the ratio method (see e.g. [7]) was used to find an independent measure of cumulants for some experiments. Crystalline bulk samples of polycrystalline Ag were used as reference standard. The EXAFS oscillations at temperature T including the contributions of all atoms used can be summarized as [8,9]

$$\chi(T,k) = \sum A\ (T,k)\sin\Phi\ \ (T,k), \tag{1}$$

where the phase of the path contribution and its amplitude are given by

$$\Phi(T,k) = 2k\left[R(T) - \frac{2C_2(T)}{R(T)}\left(1+\frac{R(T)}{\lambda}\right)\right] - \frac{4}{3}k^3 C_3(T) + \varphi(k) \text{ and} \tag{2}$$

$$A(T,k) = \frac{NS_0^2 |\, f_{eff}(k)\,|}{kR(T)^2}\exp\left(-\frac{2R(T)}{\lambda} - 2k^2 C_2(T) + \frac{2}{3}k^4 C_4(T)\right). \tag{3}$$

Here, k is the wave number of the photoelectrons ejected, N is the number of neighbours within the coordination sphere at distance $R(T)$. The quantity S_0^2 takes into account many-body effects, $f_{eff}(k)$ describes the characteristic backscattering amplitudes of neighbouring atoms, the inelastic electron scattering is described by the photoelectron mean free path λ and $\varphi(k)$ is the total phase shift.
If there exists static structural disorder, i. e. a deviation from crystalline order in the bulk of the face centered cubic (fcc) Ag lattice, e.g., at the interface of Ag nanoparticles to the glass matrix, the experimental Debye-Waller factor of the first Ag-Ag coordination sphere can be represented as superposition of a static part σ_s^2 and a dynamic one σ_d^2 according to $\sigma^2 = \sigma_s^2 + \sigma_d^2$. To separate the temperature-independent contribution σ_s^2 characterizing the static disorder and the temperature-dependent Debye-Waller factor σ_d^2 describing the harmonic lattice vibrations, the Einstein model modified by first-order perturbation can be used to calculate σ_d^2 [10-12]

$$\sigma_d^2 = \frac{\hbar^2}{2m_r k_B \Theta_E}\frac{(1+z)}{(1-z)} \qquad \text{with } z = exp\ (-\theta_E/k_B T), \tag{4}$$

where m_r is the reduced mass of the Ag-Ag pair, k_B the Boltzmann constant und θ_E the Einstein temperature. Thus, besides the usual temperature dependence, the experimental Debye-Waller factor depends on σ_s^2 and θ_E only, which can be calculated by a fit of experimental data with equ. (4).

3. Results and discussion

The EXAFS spectra measured at the Ag K-edge of glass samples containing Ag nanoparticles allowed to calculate the cumulants according to (1) – (3) for nanoparticles of 4 and 7 nm size in the tempera-

ture range between 10 and 800 K and for sizes between 1.5 and 3.5 nm in the range of 10 – 300 K, respectively. For the smaller particles, the signal-to-noise ratio was not sufficient to estimate the structural parameters at elevated temperatures (> 300 K) precisely because of both, the low amount of crystalline Ag species incorporated into nanoparticles and the increasing Debye-Waller factors in this temperature range. In figure 1 one example of Fourier transform of glass with a relatively short duration of ion exchange at 330°C (200 hours) is shown. Here, crystalline clusters or particles of 1.5 nm are formed according to TEM investigations. Besides the Ag-Ag correlations, there are also Ag-O correlations present reflecting the oxygen environment of silver ions first diffusing into the glass matrix during the ion exchange process. Subsequently, reduction of silver ions and precipitation of metal nanoparticles take place. The ratio of Ag^+ to Ag^0 is determined by the concentration of reducing agents and depends on process duration. Therefore, the fit procedures have to include this oxygen environment for all spectra measured for glass. Here, we discuss only the parameters of Ag-Ag correlations of nanoparticles.

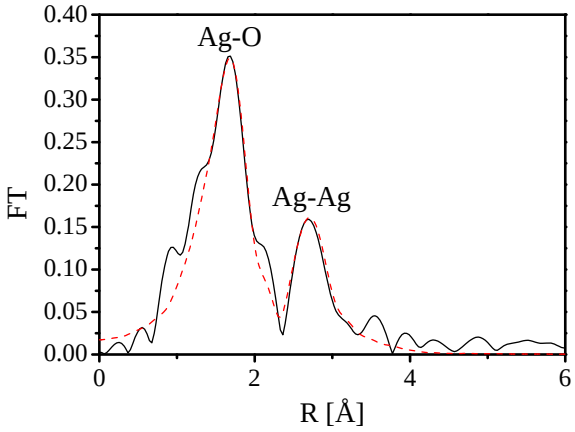

Figure 1. Ag K-edge EXAFS at 10 K for ion-exchanged glass containing particles of 1.5 nm. The dashed line represents the result of fitting.

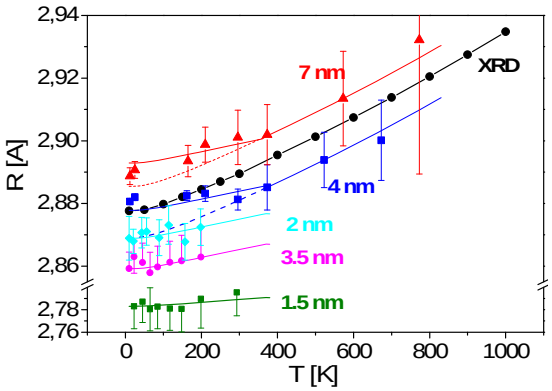

Figure 2. Ag-Ag bond lengths of nanoparticles compared with XRD data of single-crystalline Ag (lines calculated by equ. (6)).

The Ag-Ag first-shell atomic distances R as a function of temperature of different nanoparticles are compared to the corresponding XRD data of single-crystalline silver [13] in figure 2. Usually, despite the uncertainty of EXAFS analysis, the Ag-Ag lattice parameters determined by this method are always larger than the distances between the centers of probability functions measured by XRD [14]. However, this difference in bond lengths could be attributed to the effect of mean-squared vibrational disorder perpendicular to the line between the average position of the observed pair of atoms, $\langle u_\perp^2 \rangle$ [15,16]. In a previous work [12], we could show that this assumption is valid also for the crystalline lattice of Ag according to

$$R_{XRD} \approx R(T) - \frac{\langle u_\perp^2 \rangle}{2R^0} \qquad (5)$$

if the relation $\langle u_\perp^2 \rangle = 2.2 \langle u_{II}^2 \rangle$ has been used. R^0 represents the equilibrium distance. Therefore, we introduced a corresponding correction for the R(T) data of 4 and 7 nm particles, respectively. Accordingly, the number of Ag shells of these particles has been calculated. This yields the ratio of surface to interior atoms of such particles. Assuming that the vibrational behaviour of surface atoms cannot be described by (5), only the volume or interior atoms were considered for this correction. That means, in a first approximation the perpendicular vibrations were neglected for surface atoms and, concerning the lattice vibration, the interior atoms behave like atoms in crystalline bulk silver. This

correction has not been used for smaller particles (1.5, 2 and 3.5 nm) because the corresponding variations of the low-temperature atomic distances are within the experimental errors.

From the measurements represented in figure 2, an Ag-Ag distance 3.4% less than that of bulk Ag was calculated for nanoparticles of 1.5 nm in size. This value cannot be explained by the lattice contraction of small particles alone, but requires to consider the presence of Ag structures similar to those found in oxidic materials. In fact, such strongly reduced Ag-Ag distances can be found in crystalline silver oxides, for example at 2.751 Å in Ag_6O_2 [17,18]. Therefore, we assumed the formation of silver oxide-like clusters as precursors in the formation of crystalline Ag nanoparticles. The origin of Ag-Ag correlations detected by EXAFS may be due to structural units similar to Ag_6^{+4} species in oxidic structures. For larger particles, such considerable changes do not appear. Here, only a slight shift of R(T) values is found, possibly caused by thermal treatment at elevated temperatures (2 nm: 410°C; 3.5 nm: 480°C (7 h); 4 nm: 480°C (384 h); 7 nm: 600°C). Thus, we have to expect modifications of the glass structure which would influence the interaction between matrix and metal nanoparticles. Furthermore, the effect of surface or interface stress of nanospheres on the resulting Ag-Ag distance of nanoparticles can be discussed.

Obviously, the dependence of Ag-Ag distances on temperature shows a two-range behaviour. At low temperatures, there is a considerably lower increase with temperature than in the high-temperature range (> 400 K) for the larger particles of 4 and 7 nm. These data are obtained independent of the course of temperature during the experiments. Usually, such effects occur above the glass transformation temperature. However, this temperature is at about 807 K. Nevertheless, this effect can be ascribed to a temperature-dependent interaction between nanoparticles and the surrounding glass matrix. Here, a critical temperature, T_C, of approximately 400 K must be assumed in relation to a thermoelastic model. This model explains that effect by the strong difference of thermal expansion coefficients of Ag nanoparticles and the glass matrix. The thermal expansion coefficient of Ag is three times larger than that of the soda-lime glass. Thus, the thermal expansion of the nanoparticles below T_C is hindered by the glass matrix, whereas above this temperature a relaxation at the nanoparticle-glass interface takes place. This gives an effective coefficient of the particles below T_C to be α_{Ag} - α_{glass}. Applying Eshelby's solution for a spherical defect in an infinite medium [19], the relative change of Ag-Ag distance *R(T)* of Ag particles below T_C is given by

$$\frac{\Delta R}{R} = \left(4\lambda G_m\right)^{-1} \int_{T_C}^{T} \left(\alpha_p(T') - \alpha_m(T')\right) dT' \; ; \; \lambda = \frac{1+\nu_m}{2E_m} + \frac{1-2\nu_p}{E_p} . \qquad (6)$$

Here, the material properties E (Young'modulus), ν (Poisson's ratio), α (thermal expansion coefficient) and G (shear modulus) have to be considered. The subcripts m and p refer to the glass matrix and the particle, respectively. Using (6), the nanoparticles are subjected to a tensile stress below T_C and their effective expansion decreases as shown by the calculated line in figure 4. At temperatures above T_C there exists no such hinderance and the particles of 4 and 7 nm size show an expansion similar to that of bulk silver. In this case, no size effects of nanoscaled species could be observed.

Additional information on thermal vibration and disorder in nanoparticles is available from EXAFS spectra by the second cumulant $\sigma^2 = C_2$. One example is given in figure 3. The results for all particle sizes are summarized in figures 4a and b. The comparison with the data of the polycrystalline foil demonstrates that static disorder inside the particles increases with decreasing particle sizes, especially, below 5 nm sizes. This distinctly higher Debye-Waller factor indicates a larger static disorder due to the high number of surface atoms of such particles or clusters. On the other hand, in case of extended duration of ion exchange or a subsequent thermal treatment, i. e. for larger particles, the Ag-Ag distance is similar or slightly larger than that of bulk silver and the Debye-Waller factor decreases. There are already some results of EXAFS experiments which point to an increase of static disorder for small particles as well as of

ion irradiation of Au nanoparticles [20-22]. In the case of embedded particles, besides the size effect, the interactions with the matrix must be taken into consideration. Here, both effects should be reflected by the EXAFS results. The structural mismatch of glass matrix and metal particles should increase the static disorder. For small sizes of particles, the Einstein temperature increases. That should be due to changes of the bond character, maybe, in correlation to decreasing Ag-Ag bond lengths as shown above. Similar results have been found for Te or Cu nanoparticles [23, 24]. The drastic increase of static disorder and Θ_E of 1.5 nm particles seems to confirm the size effect observed for larger particles. However, the effect of oxidic structures on EXAFS cumulants should be determined in further investigations.

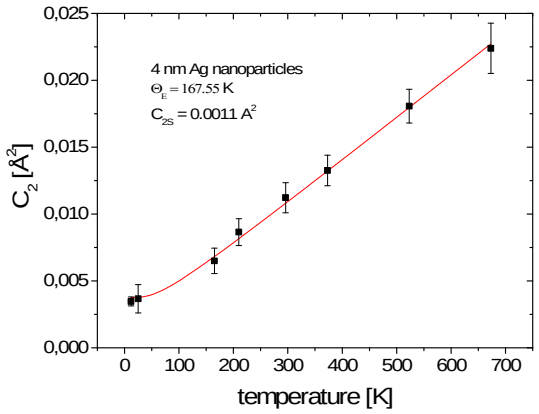

Figure 3. Experimental data of Debye-Waller factor of 4 nm particles. The fit yields a static part σ_s^2 of 0.0011 Å^2 and a dynamic part using (4) with an Einstein temperature of 167.55 K.

Finally, it should be mentioned that the third-order cumulants show a similar increase for small Ag particles as the Debye-Waller factor. A detailed discussion of this result requires the development of theoretical interpretation of cumulant expansion in relation to potential functions (see for example [22,25,26]). The quality of data of fourth cumulants does not allow a systematic discussion for most of the particles.

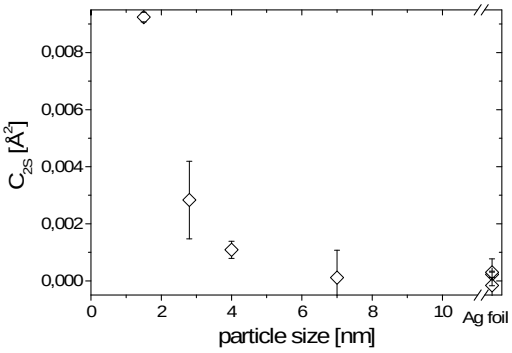

Figure 4a. Results of data evaluation concerning the static Debye-Waller factor $C_{2,s}$.

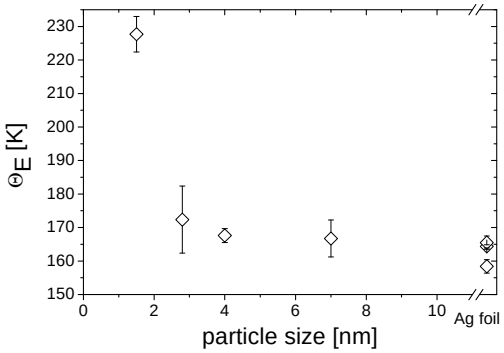

Figure 4b. Einstein temperature as function of particle size.

4. Conclusions

The formation of Ag nanoparticles in soda-lime glass by ion exchange procedure starts with Ag clusters that contain oxidic structures as precursor states for precipitation of pure Ag particles. The measured Ag-Ag bond length of nanoparticles are governed by the existence of such precursor

configurations, by surface or interface effects and by the interaction between the glass matrix and the metal particles. The latter causes a hindered contraction of Ag particles and a formation of tensile stresses below a critical temperature of about 400 K. Above T_C, the thermal expansion of larger particles is similar to that of bulk material. This interaction is near to the limit of using the continuum elasticity theory. The vibrations of atoms are characterized by an increased Einstein temperature for decreasing particle size. A distinct disorder has been noticed inside the particles, especially, for very small sizes.

References

[1] Gonella F and Mazzoldi P 2000 *Handbook of Nanostructured Materials and Nanotechnology*, vol 1 (London: Academic Press) metal nanoparticles, applications
[2] Diaz-Moreno S, Koningsberger D C and Munoz-Paez A 1997 *Nucl. Instr. & Meth. Phys. Res. B* **133** 15
[3] Bazin D and Rehr J J 2003 *J. Chem. Phys. B* **12** 398
[4] Dubiel M, Haug J, Kruth H, Hofmeister H and Schicke K-D 2008 *Mat. Sc. Eng. B* **149** 146
[5] Zabinsky S I, Rehr J J, Ankudinov A, Albers R C and Eller M J 1995 *Phys. Rev. B **52** 2995-3009*
[6] Ankudinov A L, Nesvizhskii A I and Rehr J J 2003 *Phys. Rev. B* **67** 115120
[7] Bunker G 1983 *Nucl. Instrum. Methods Phys. Res.* **207** 437
[8] Rehr J J and Albers 2000 *Rev. Mod. Phys.* **72** 621
[9] Freund J, Ingalls R and Crozier E D 1989 *Phys. Rev. B* **39** 12537
[10] Sevillano E, Meuth M and Rehr J J 1979 *Phys. Rev. B* **20** 4908
[11] Tröger L, Yokoyama T, Arvanitis D, Lederer T, Tischer M and Baberschke K 1994 *Phys. Rev. B* **49** 888
[12] Haug J, Chassé A, Schneider R, Kruth H and Dubiel M 2008 Phys. Rev. B 77 184115
[13] Touloukian y S, Kirby R K, Taylor R E and Desai 1975 *Thermophysical Properties of Matter* (Plenum, New York) **12** 298
[14] Dalba G, Fornasini P, Gotter R and Rocca F 1995 *Phys. Rev B* **52** 149
[15] stern E A 1997 *J. Phys.* **IV 7** C2-137
[16] Dalba G, Fornasini R, Grisenti R, Pasqualini D, Diop D and Monti F 1998 *Phys. Rev. B* **58** 4793
[17] Jansen M 1987 *Angew. Chemie* **99** 1136
[18] Dubiel M, Schneider R, Hofmeister H, Schicke K-D and Pivin J C 2007 *Eur. Phys. D* **43** 291
[19] Miyata N and Jinno H 1981 *J. Mater. Sci.* **16** 2205
[20] Kuroda H, Yokoyama T, Asakura K and Iwasawa Y 1991 *Faraday Discuss.* **92** 189
[21] Johannessen B, Kluth P, Llewellyn D J, Foran G J, Cookson D J and Ridgway M C 2007 *Phys. Rev. B* **76** 184203
[22] Kluth P et al. 2006 *Phys. Rev. B* **74** 014202
[23] Ikemoto H and Miyanaga T 2007 *Phys. Rev. Lett.* **99** 165503
[24] Ceolin M, Galvez N and Dominguez-Vera J M 2008 *Phys. Chem. Chem. Phys.* **10** 4327
[25] Vila F D, Rehr J J, Rossner H H and Krappe H J 2007 *Phys. Rev. B* **76** 014301
[26] Comaschi T, Balerna A and Mobilio S 2008 *Phys. Rev. B* **77** 075432